Inorganic Chemistry
Communication

Inorg. Chem. **2010**, *49*, 6787–6789 **6787**
DOI: 10.1021/ic100785r

Metal-Interrupted Perylene Diimide: Toward a New Class of Tunable n-Type Inorganic−Organic Hybrid Semiconductors

Kate R. Edelman and Bradley J. Holliday*

Department of Chemistry and Biochemistry and Center for Electrochemistry, The University of Texas at Austin, 1 University Station, A5300, Austin, Texas 78712-0165

Received April 27, 2010

In organic thin-film transistors (OTFTs), organic electron-transport materials (n-type semiconductors) are well behind the advances in development of hole-transport materials (p-type semiconductors). Currently, one class of organic n-type semiconductor materials that is widely utilized is *N,N′*-dialkyl-3,4,9,10-perylenetetracarboxylic diimide (PTCDI-R) derivatives with high electron affinities (EAs), such as *N,N′*-dioctyl-3,4,9,10-perylenetetracarboxylic diimide with a reported EA as high as 4.4 eV. The PTCDI-R derivatives have been manipulated by adding substituents on the perylene moiety or at the amine position to afford more stable compounds and higher EAs. On the basis of these materials, we have developed metal-containing perylenediimide analogues, placing a salpen ligand for metal ion chelation between two *n*-isobutylnaphthalimides. We demonstrate here that the electronic properties of this class of materials can be systematically tuned in a divergent manner by simply changing the metal center. The synthesis, characterization, electrochemistry, and band-gap analysis are discussed herein.

Organic semiconductors were identified as early as 1940, but low charge mobilities hindered the development of practical applications of these materials. It was not until the late 1980s when work on organic thin-film transistors (OTFTs) reignited research on both polymer- and small-molecule-based organic electronics.[1−3] Organic materials are advantageous over the inorganic counterparts because of their ability to create flexible devices that can be produced on a large scale and at relatively low cost.[4]

While a wide variety of organic hole-transport materials (p-type semiconductors) for applications such as OTFTs have been successfully developed, electron-transport materials (n-type semiconductors) still have to overcome many challenges. When highly charged, organic n-type materials are reactive toward oxygen and moisture, thus making it difficult to create robust OTFTs, which perform well when doped. In addition, improving electron injection and transport in organic devices requires materials with high electron affinities (EAs).[5,6] Specifically, organic transistors require EA values of about 4.0 eV or higher to create ohmic contacts to aluminum electrodes and even higher for gold electrodes.[7,8] Finally, tuning of the EA of organic semiconductors usually involves the addition of electron-withdrawing substituents (i.e., −CN or F), and this often requires lengthy tedious synthetic procedures.

To date, examples of organic n-type materials with high EAs include hexadecafluorocopper phthalocyanine (F_{16}CuPc) and *N,N′*-dialkyl-3,4,9,10-perylenetetracarboxylic diimide derivatives. The EA value for F_{16}CuPc is 3.4 eV, and that of *N,N′*-dioctylperylene-3,4,9,10-tetracarboxylic diimide (PTCDI-C_8) is 4.4 eV.[9,10] The perylene diimides are of particular interest not only because of high EAs but also because of the fact that the electronic properties can be tuned in a rational way through synthetic manipulations of the substituents around the aromatic core.[11,12] Herein, we describe a new class of materials with the potential for use as n-type organic electronics whereby a perylene diimide aromatic structure is interrupted by a Schiff-base metal complex (Scheme 1). This strategy has been developed, in part, to take advantage of the ability to tune the electronic properties of these complexes by simply changing the metal center.

Our approach to developing metal-containing perylene diimide analogues (Scheme 1) involves placing a salpen ligand (salicyaldehydes connected through a 1,3-propylenediamine backbone) between two naphthalimide moieties with

*To whom correspondence should be addressed. E-mail: bholliday@cm.utexas.edu.

(1) Horowitz, G. J. *Mater. Res.* **2004**, *19*, 1946.
(2) *Organic Electronics: Materials, Manufacturing and Applications*; Klauk, H., Ed.; Wiley-VCH: New York, 2006.
(3) Newman, R. C.; Frisbie, C. D.; da Silva Filho, D. A.; Bredas, J.-L.; Ewbank, P. C.; Mann, K. R. *Chem. Mater.* **2004**, *16*, 4436.
(4) *Organic Field-Effect Transistors*; Bao, Z., Locklin, J., Eds.; CRC Press: Boca Raton, FL, 2007.
(5) Bao, Z.; Lovinger, A. J.; Dodabalapur, A. *Appl. Phys. Lett.* **1996**, *69*, 3066.
(6) Babel, A.; Jenekhe, S. A. *Adv. Mater.* **2002**, *14*, 371.
(7) Sirringhaus, H.; Tessler, N.; Friend, R. H. *Science* **1998**, *280*, 1741.
(8) Zhu, Y.; Yen, C.-T.; Jenekhe, S. A.; Chen, W.-C. *Macromol. Rapid Commun.* **2004**, *25*, 1829.
(9) Hosoi, Y.; Tsunami, D.; Ishii, H.; Furukawa, Y. *Chem. Phys. Lett.* **2007**, *436*, 139.
(10) Kim, K.; Kwak, T. H.; Cho, M. Y.; Lee, J. W.; Joo, J. *Synth. Met.* **2008**, *158*, 553.
(11) Chesterfield, R. J.; McKeen, J. C.; Newman, C. R.; Ewbank, P. C.; da Silva Filho, D. A.; Bredas, J.-L.; Miller, L. L.; Mann, K. R.; Frisbie, D. C. *J. Phys. Chem.* **2004**, *108*, 19281.
(12) Liang, B.; Zhang, Y.; Wang, Y.; Xu, W.; Li, X. *J. Mol. Struct.* **2008**, *917*, 133.

Published on Web 06/29/2010

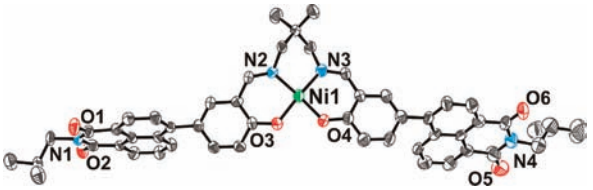

Figure 1. ORTEP diagram of **5** showing the labeling scheme of selected atoms with thermal ellipsoids drawn at the 30% probability level. Hydrogen atoms and solvent molecules are omitted for clarity.

Scheme 1. Synthetic Scheme for Bis(isobutylnaphthalimide)salpen Metal Complexes[a]

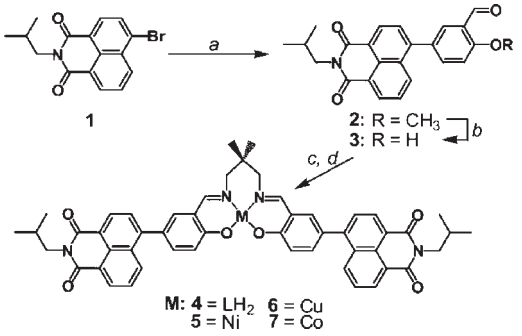

[a] (a) 3-Formyl-4-methoxybenzeneboronic acid, Na_2CO_3, $PdCl_2(PPh_3)_2$, dry DMF. (b) 1.0 M BBr_3 in CH_2Cl_2, dry CH_2Cl_2. (c) 2,2-Dimethylpropane-1,3-diamine, EtOH, CH_2Cl_2. (d) $M(OAc)_2 \cdot xH_2O$, EtOH, CH_2Cl_2.

isobutyl groups used to improve the solubility. The salpen moiety was chosen because of its ease of metalation as well as evidence that there is electronic communication through the salen bonds to the metal in conducting metallopolymer systems.[13−15] By variation of the metal center, the relative redox properties of the naphthalimide, in conjunction with these metal centers, will be affected and studied. We have chosen to specifically study nickel(II) (**5**), copper(II) (**6**), and cobalt(II) (**7**) because of the II → I redox couples previously reported for the respective salen complexes (vide infra).

The metalated salpen isobutylnaphthalimide complexes (**5**−**7**, Scheme 1), as well as the precursors (**1**−**4**), have been synthesized and fully characterized by ^1H and ^{13}C NMR spectroscopy (when practical), mass spectrometry, UV−vis spectroscopy, cyclic voltammetry, and combustion analysis, and all data are fully consistent with the proposed structures. The solid-state structure of the nickel(II) metal complex (**5**) was also determined by single-crystal X-ray diffraction analysis (Figure 1).[15] This analysis reveals several interesting features about complex **5**. The four-coordinate Ni^{II} center is in a twisted square-planar geometry (28.14°) that is defined by the two nitrogen atoms and two oxygen atoms from the salpen ligand. The Ni−N_{av} bond distance (1.882 Å) is longer than the Ni−O_{av} bond distance (1.842 Å). This trend and these bond distances are consistent with a previously reported crystal structure of a nickel(II) salen complex (Ni−N_{av} = 1.871 Å; Ni−O_{av} = 1.846 Å).[16] The phenyl and naphthalimide ring planes are twisted with respect to each other, with the torsion angles between the two moieties being 55.79° for the left side of the molecule and 66.22° for the right side, as displayed in Figure 1. A torsion angle of 21.94° is observed between the individual naphthalimide rings.

Table 1. λ_{max} Values, Solution Reduction Potentials, Derived LUMO and HOMO Energies, and Band-Gap Analysis

	λ_{max}[a]	$E_{1/2\ (red.)}$[b]	E_{LUMO}[c]	E_{HOMO}[c]	band gap[c]
4	229, 369	−1.90	−3.12	−5.50	2.38
5	236, 427	−1.93	−3.19	−5.03	1.84
6	236, 410	−1.86	−3.38	−5.37	1.99
7	235, 407	−1.85	−3.71	−5.21	1.50

[a] In nm. [b] Volts vs Fc/Fc^+. [c] Electronvolts vs vacuum.

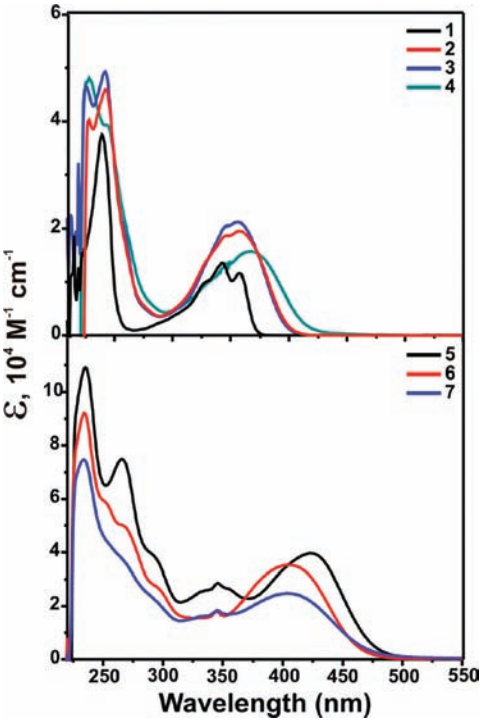

Figure 2. UV−vis absorption spectra of **1**−**7** in DCM at room temperature.

The electronic absorption spectra of **1**−**7** have been studied in dichloromethane (DCM) at room temperature. The λ_{max} values for **4**−**7** are displayed in Table 1. The absorption spectra of **1**−**4** display two broad bands from 225 to 285 nm and from 300 to 400 nm (Figure 2, top). The absorption maxima (λ_{max} = ∼238 nm) of **1**−**4** are attributed to a $\pi \rightarrow \pi^*$ transition of the salicylaldehyde moiety, and the second displayed absorption maxima (λ_{max} = ∼358 nm) are attributed to a $\pi \rightarrow \pi^*$ transition of the naphthalimide moiety.[17,18] The absorption spectra of **5**−**7** display three broad bands: from 225 to 305 nm, from 300 to 375 nm, and from 380 to 470 nm (Figure 2, bottom). The two higher-energy absorption maxima (λ_{max} = ∼236 and ∼350 nm) of **5**−**7** are again attributed to $\pi \rightarrow \pi^*$ transitions from the salpen and naphthalimide moieties, respectively, while the new lower-energy absorption maxima (λ_{max} = ∼414 nm) are

(13) Kingsborough, R. P.; Swager, T. M. *Adv. Mater.* **1998**, *10*, 110.
(14) Kingsborough, R. P.; Swager, T. M. *J. Am. Chem. Soc.* **1999**, *9*, 8825.
(15) Crystal data for **5**: $C_{51}H_{46}N_4NiO_6 \cdot C_3H_7NO \cdot H_2O$, M = 960.74, triclinic, space group $P\bar{1}$, a = 9.6700(4) Å, b = 14.0580(7) Å, c = 18.1070(10) Å, α = 107.225(2)°, β = 94.799(3)°, γ = 104.624(2)°, V = 2241.24(19) Å^3, Z = 2, D_{calcd} = 1.424 g cm^{-3}, μ = 0.498 mm^{-1}, T = 153(2) K, R1 = 0.1727, R2 = 0.2209.
(16) Cengiz, A.; Filiz, E.; Kurtaran, R.; Atakol, O. *Acta Crystallogr., Sect. C: Cryst. Struct. Commun.* **2001**, *C57*, 812.
(17) Wintgens, V.; Valat, P.; Kossanyi, J. *New J. Chem.* **1996**, *20*, 1149.
(18) Nandhikonda, P.; Begaye, M. P.; Cao, Z.; Heagy, M. D. *Chem. Commun.* **2009**, 4941.

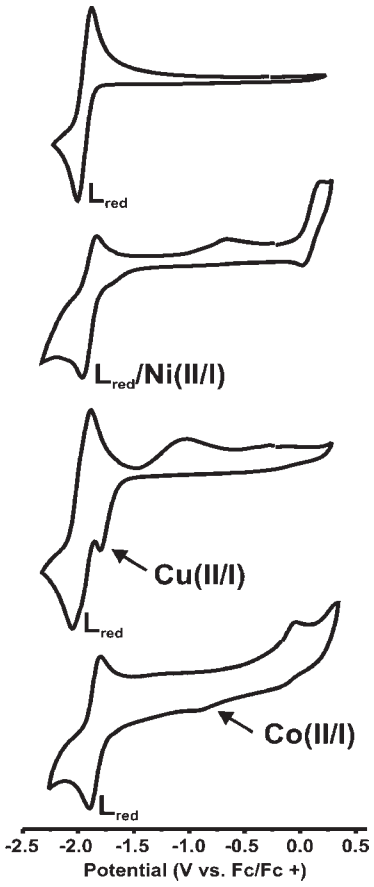

Figure 3. Cyclic voltammograms of compounds **4**−**7**.

attributed to M → L charge-transfer transitions, which was confirmed by solvatochromism (see the Supporting Information).[19]

In order to determine the EA of the salpen isobutylnaphthalimide materials, the electrochemical properties were investigated. Cyclic voltammetry was performed over a window of +0.50 to −2.05 V (vs Fc/Fc^+) at a scan rate of 100 mV/s in anhydrous dimethylformamide (DMF) to determine the reduction potentials of the various compounds. Additionally, separate cyclic voltrammetry experiments were performed over a window of −0.5 to +1.5 V (vs Fc/Fc^+) at a scan rate of 100 mV/s in anhydrous DCM to locate the onset of oxidation for band-gap analysis. The ligand (**4**) shows a reversible reduction wave with $E_{1/2}$ = −1.90 V (Figure 3). With this information, metals were chosen according to how well the redox couples of these metal ions in salen ligands overlapped with the reduction potential of **4**. By varying the electrochemical overlap, we can examine what role the metal might play in the realized electronic properties of the materials and how its redox chemistry in relation to the ligand affects the realized EA. From previous literature reports, the nickel(II/I) salen redox couple is $E_{1/2}$ = −1.69 V, which should create overlap with the redox couple of the flanking organic groups, the copper(II/I) salen redox couple is $E_{1/2}$ = −1.27 V, which should not overlap well, and the cobalt salen redox couple is $E_{1/2}$ = −0.58 V, which should have absolutely no overlap with the ligand redox couple.[20−23]

Cyclic voltammetry of **5** illustrates a slight shift of the reversible reduction to $E_{1/2}$ = −1.93 V and displays good overlap between the metal and ligand reduction potentials. Complex **6** overlaps more than predicted, with a peak at −1.76 V that is associated with the reduction of copper from copper(II) to copper(I), while the ligand redox couple displays a shift to $E_{1/2}$ = −1.86 V. The cobalt complex **3** shows two well-separated redox couples: one that is ligand-based at $E_{1/2}$ = −1.85 V and one that is metal-based at −0.80 V, corresponding to the cobalt(II/I) redox couple.

The EAs [lowest unoccupied molecular orbital (LUMO) level] of **4**−**7**, estimated from the onset of the reduction potential by conversion to SCE and taking the SCE energy level to be −4.8 eV relative to the vacuum level (EA = $E_{\text{onset red}}$ + 4.8), are 3.12, 3.19, 3.38, and 3.71 eV, respectively.[24] These EA values are comparable with F_{16}CuPc values but are lower than the value reported for PTCDI-C_8 (vide supra).

Band-gap analysis, i.e., determination of the highest occupied molecular orbital (HOMO) and LUMO positions, is necessary for determining the majority of charge carriers and inferring the stability of the charge carrier in organic semiconductors. HOMO and LUMO levels were calculated from the onset of oxidation and reduction in the electrochemical data for complexes **4**−**7** with respect to the vacuum level (Table 1).[24] The band gaps appear to be on the same order as those of several previously reported peryelene derivatives studied for photovoltaic devices by Shin et al.[25] The calculated band gaps for **4**−**7** are 2.38, 1.84, 1.99, and 1.50 eV, respectively.

In summary, we have synthesized and characterized a series of metal-containing perylene diimide analogues and fully investigated their electrochemical behavior. These complexes exhibit EAs comparable to those of n-type materials currently used in OTFT fabrication. With further investigation and manipulation of the ligand structure in the future, we plan to try to tune the electronics of this potential new class of hybrid semiconductors to improve upon the obtained EAs.

Acknowledgment. We gratefully acknowledge the Welch Foundation (F-1631), the PRF/ACS (47022-G3), the NSF (CHE-0639239, CHE-0741973, and CHE-0847763), the THECB (ARP 003658-0010-2006), the UT-CNM, The National Institute for Nano-Engineering (NINE) Program at Sandia National Laboratories, and UT-Austin for supporting this research.

Supporting Information Available: Experimental details for the synthesis and characterization of **1**−**7**, electrochemical data for **1**−**4**, a solvatochromism UV−vis study of **5**, X-ray diffraction tables, and crystallographic data for **5** in CIF format. This material is available free of charge via the Internet at http://pubs.acs.org.

(19) Bella, S. D.; Fragala, I.; Ledoux, I.; Diaz-Garcia, M. A.; Marks, T. J. *J. Am. Chem. Soc.* **1997**, *119*, 9550.
(20) Fritzche, S.; Lonnecke, P.; Hocher, T.; Hey-Hawkins, E. *Z. Anorg. Allg. Chem.* **2006**, *632*, 2256.
(21) Gach, P. C.; Karty, J. A.; G., P. D. *J. Electroanal. Chem.* **2008**, *612*, 22.
(22) Hoferkamp, L. A.; Goldsby, K. A. *Chem. Mater.* **1989**, *1*, 348.
(23) Kingsborough, R. P.; Swager, T. M. *Chem. Mater.* **2000**, *12*, 872.
(24) Tonzola, C. J.; Alam, M. M.; Jenekhe, S. A. *Adv. Mater.* **2002**, *14*, 1086.
(25) Shin, W. S.; Jeong, H.-H.; Kim, M.-K.; Jin, S.-H.; Kim, M.-R.; Lee, J.-K.; Lee, J. W.; Gal, Y.-S. *J. Mater. Chem.* **2006**, *16*, 384.